# Continuous-Time Switched H∞ Proportional-Integral observer: Application for sideslip and road bank angles estimation

Lghani Menhour, Damien Koenig, Brigitte D 'Andréa-Novel

# Continuous-Time Switched $H_\infty$ Proportional-Integral Observer: Application for Sideslip and road bank angles estimation

Lghani Menhour, Damien Koenig and Brigitte d'Andréa-Novel

***Abstract*— In this work, a Continuous-Time Switched $H_\infty$ Proportional-Integral (CTS$H_\infty$PI) observer is presented. The estimation method is based on a proportional-integral observer introduced by [13], [11], [12]. The estimation method is used to estimate simultaneously the state variables and unknown inputs of switched systems. A design method is established using a common Lyapunov function and $H_\infty$ norm. Its stability and global convergence conditions are proved and expressed in term of LMIs. All conditions are established under given switching signals. The estimation method is applied in vehicle dynamics to estimate simultaneously the vehicle sideslip angle and road bank angle. Moreover, the switching signal is deduced from measured premise variables. Simulation tests with experimental data are included to demonstrate the advantage of this method.**

***Keywords*: Switched PI observer, Switched systems, stability, $H_\infty$-filtering, LMI, vehicle application.**

## I. Introduction

The development of efficient intelligent systems like intelligent transportation systems requires the knowledge of the vehicle models, for example control and estimation algorithms. Indeed, the design of such algorithms to estimate the dynamical parameters and some unknown inputs, requires the adequate models. However, the knowledge of these models is generally poor and local. Consequently, to overcome such a constraint and improve these models, several solution are developed among which the switched systems. The switched systems have been introduced recently [15], [14], [6], [2], [4], [16], [25], [19], [18], [17], [22], [7] and are an important class of hybrid systems. Such systems are defined by a finite number of subsystems and a switching rule that orchestrates switching between them, in other words, the switching rule is generally employed to activate the corresponding subsystem.

Several investigations on analysis and synthesis of such systems under arbitrary switching signals are conducted [16], [25], [19] and the references cited therein. In particular, the stability analysis of switching linear systems is widely addressed by using switched Lyapunov functions [15], [6], [2], [4] and a common quadratic Lyapunov function [16], [25], [19], [18]. In several cases, the stability analysis in the Lyapunov sens allows to develop design methods via LMI optimization with $H_\infty$ norm performance. Such a approach is used to design several control and estimation algorithms like those presented in [15], [14], [4].

The aim of this study is to propose a continuous-time switched observer to estimate simultaneously the vehicle dynamics states and unknown input. The use of switched systems is due to the simplicity of lateral tire force models, road conditions and longitudinal speed variation. In order to design efficient safety systems to improve the stability and the steerability of the vehicle, an accurate estimation of some parameters (like sideslip angle) and unknown inputs (like road bank angle) is required. Moreover, the measurements provided by low cost sensors like a lateral accelerometer and a yaw rate gyrometer are affected considerably by a road bank angle. The road bank angle play a crucial role on maximal achievable velocity in a bend. Concerning the sideslip angle, it is also used in the existence safety systems like ESP, and its estimation allows us overcome the use of more expensive sensors like Correvit sensor (around 15 K€).

The sideslip and road bank angles estimation problems have been already treated in several works like in [9], [8], [23], [21], [28], [10], [5], [3], [24], [1]. Some of these works assume that the vehicle model parameters are well known which is not generally the case. Moreover, the spectral domain of the road bank angle is in low frequency range and can be considered as an unknown input, then, its estimation can be performed by a PI observer [13], [11], [12]. In order to increase the estimation performance, a switched PI observer strategy is used. This method takes also advantage of common Lyapunov function design method [16], [25], [19], [18] and $H_\infty$ norm [6], [26], [27], [14]. This, in order to guarantee an appropriate estimation of sideslip and road bank angles, whatever the parameter variations, like tire cornering stiffnesses and longitudinal speed.

The remainder of the paper is organized as follows. In Section II, a lateral vehicle model and design problem of CTS $H_\infty$ PI Observer are presented. Design observer method and its proof are established in Section III. A validation results using the experimental data are presented in Section IV. In section V, conclusions and perspectives are given.

## II. Vehicle model and switched estimation problem

### A. Single-track vehicle model

The bicycle vehicle model used in this study is composed of three degrees-of-freedom: sideslip, yaw and roll motions.

This work was supported by the French national project INOVE/ANR 2010 BLANC 308.

L. Menhour is with Centre de Recherche STIC, IUT de Troyes, 9, Rue du Québec, 10000 Troyes, France lghani.menhour@univ-reims.fr

D. Koenig is with Laboratoire de Grenoble Images Parole Signal et Automatique, UMR CNRS-INPG-UJF, 38402 Saint Martin d'Hres, France Damien.Koenig@gispa-lab.grenoble-inp.fr

B. d'Andréa-Novel is with Mines-ParisTech, CAOR-Centre de Robotique, Mathématiques et systèmes, 60 boulevard Saint-Michel, 75272 Paris cedex 06, France brigitte.dandrea-novel@mines-paristech.fr

The state representation of this model is as follows:

$$\left\{\begin{array}{l} \dot{x} = Ax(t) + Bu(t) + F\omega(t) \\ y = Cx(t) \end{array}\right. \quad (1)$$

where: $A = \begin{bmatrix} -\frac{I_{eq}C_{\alpha,0}}{I_x m V_x} & -1-\frac{I_{eq}C_{\alpha,1}}{I_x m V_x^2} & \frac{C_{\alpha,3}}{I_x V_x} & -\frac{h_r L_r}{I_x V_x} \\ -\frac{C_{\alpha,1}}{I_z} & -\frac{C_{\alpha,2}}{I_z V_x} & 0 & 0 \\ 0 & 0 & 0 & 1 \\ -\frac{C_{\alpha,0}h_r}{I_x} & -\frac{C_{\alpha,1}h_r}{I_x V_x} & \frac{mgh_r - K_r}{I_x} & -\frac{b_r}{I_x} \end{bmatrix}$, $H = \begin{bmatrix} I_e C_f / I_x m V_x(t) \\ l_f C_f / I_z \\ 0 \\ C_f / I_x \end{bmatrix}$, $C = \begin{bmatrix} 0 & 1 & 0 & 0 \\ 0 & 0 & 1 & 0 \\ 0 & 0 & 0 & 1 \end{bmatrix}$, $u = \delta$, $\omega = \phi_r$, $x = \begin{bmatrix} \beta & \dot{\psi} & \phi_v & \dot{\phi}_v \end{bmatrix}^T$, $F = \begin{bmatrix} -g/V_x(t) & 0 & 0 & 0 \end{bmatrix}^T$, $I_{eq} = I_x + mh_r^2$, $C_{\alpha,0} = C_f + C_r$, $C_{\alpha,1} = L_f C_f - L_r C_r$, $C_{\alpha,2} = L_f^2 C_f + L_r^2 C_r$ and $C_{\alpha,3} = h_r(mgh_r - K_r)$

$\omega$ is an unknown input situated in law frequency. Notice that the lateral tire forces are supposed to be proportional to sideslip angles of each axle as follows:

$$F_{yf} = C_f\left(\delta - \beta - \frac{L_f\dot{\psi}}{V_x}\right) \text{ and } F_{yr} = -C_r\left(\beta - \frac{L_r\dot{\psi}}{V_x}\right) \quad (2)$$

### B. Switched estimation: problem formulation

The simplicity of model (1), is not an advantage to have an efficient estimation of sideslip and of road bank angles. Otherwise, the parameters of such a model (1) like longitudinal speed $V_x$ and cornering stiffnesses coefficients ($C_f$ and $C_r$) vary over the time. In fact, for braking or driving maneuvers, $V_x$, $C_f$ and $C_r$ become variables. Figure 1 shows the measured lateral tire force characteristic during braking maneuver. We can observer that $C_f$ and $C_r$ have two different dynamics.

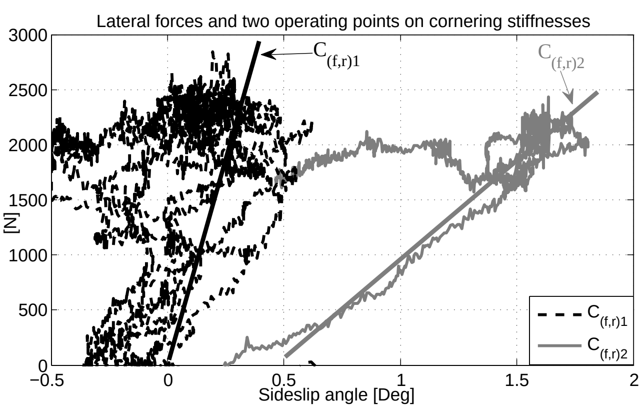


Fig. 1. Experimental lateral tire force characteristic and two operating points $C_{(f,r)_1}$ and $C_{(f,r)_2}$

To consider all these variations, the Linear Time Invariant system (1) can be transformed into a switched one. Then, system (1) can be rewritten as:

$$\left\{\begin{array}{l} \dot{x}(t) = \sum_{i=1}^{M} \alpha_i(\vartheta(t))\left[A_i x(t) + B_i u(t) + F_i \omega(t)\right] \\ y(t) = \sum_{i=1}^{M} \alpha_i(\vartheta(t)) C_i x(t) \\ \xi(t) = \sum_{i=1}^{M} \alpha_i(\vartheta(t)) L_i x(t) \end{array}\right. \quad (3)$$

where $A_i$,$F_i$, $H_i$, $C_i$, $G_i = 0$ and $L_i$ are known matrices. $x \in \mathbb{R}^n$, $\omega \in \mathbb{R}^{n\omega}$, $u(t) \in \mathbb{R}^{n_u}$ and $y \in \mathbb{R}^m$ denote respectively the state vector, the unknown input vector, the vector control and the output vector. $\xi(t) \in \mathbb{R}^r$ is the vector to be estimated, with $r \leq n$. $\alpha_i(t)$ is the switching signal given by

$$\alpha_i : \mathbb{R}^+ \longrightarrow \{0, 1\} \quad \sum_{i=1}^{M} \alpha_i(\vartheta(t)) = 1, \quad t \in \mathbb{R}^+ \quad (4)$$

where $\vartheta(t)$ is the premise variable depending on measurable variables. The objective of this study is to design a continuous-time switched H$_\infty$ PI observer which is derived from the PI observer proposed in [12]. This observer estimate simultaneously the state of the system and the road bank angle. In the following, the design problems of continuous-time switched H$_\infty$ PI observer for systems (3) is addressed.

*Problem 1:* Consider the following continuous-time switched H$_\infty$ PI observer for switched system (3)

$$\left\{\begin{array}{l} \dot{z} = \sum_{i=1}^{M} \alpha_i(\vartheta(t))\left(\Pi_i z + K_{p_i} y + T_i F_i \hat{\omega} + T_i B_i u(t)\right) \\ \dot{\hat{\omega}} = \sum_{i=1}^{M} \alpha_i(\vartheta(t))\left(K_{I_i}(y - C_i \hat{x})\right) \\ \hat{x} = \sum_{i=1}^{M} \alpha_i(\vartheta(t))\left(z + N_i y\right) \end{array}\right. \quad (5)$$

where $z \in \mathbb{R}^n$, the gains $K_{p_i}$ and $K_{I_i}$ are computed such that the following specification is ensured:

S1. the estimate $\hat{x}$ and $\hat{\omega}$ converge asymptotically to the state $x$ and the unknown input $\omega$ respectively;

S2. the optimization problem

$$\min \gamma$$

subject to

$$\left\|G(s)_{\tilde{\xi}\omega}\right\|_\infty < \gamma$$

where $\left\|G(s)_{\tilde{\xi}\omega}\right\|_\infty$ denotes the H$_\infty$ norm from $\omega(t)$ to $\tilde{\xi}(t) = \xi(t) - \hat{\xi}(t)$.

The problem of the continuous-time switched H$_\infty$ PI observer design is also reduced to finding matrices $\Pi_i$, $K_{p_i}$, $K_i$, $T_i$, $K_{I_i}$, $N_i$ for each $i$ such that S1 hold. Moreover, the spectral domain of the bank angle is in a low frequency range. Then, its estimation and the estimation of dynamical states can be performed simultaneously with such an observer. The general assumptions of [12, A1 to A4b] are reduced to:

A1:

$$rank(F_i) = n_\omega, \ rank(C_i) = m; \quad \forall i = 1, \cdots, M.$$

A2:

$$rank\left(\begin{bmatrix} pI_n - A_i & -F_i \\ 0 & pI_{n_\omega} \\ C_i & 0 \end{bmatrix}\right) = n + rank(F_i)$$
$$\forall \mathbb{R}(p) \geq 0; \quad \forall i = 1, \cdots, M.$$

*Remark 1:* Assumption A1 ensures respectively that the UI's and measurements are linearly independent. Assumption A2 ensures that the detectability properties is satisfied.

## III. Continuous-time Switched $H_\infty$ PI Observer design

In this section, we present a method to design the continuous-time switched $H_\infty$ PI observer (5) for system (3), and we state the following theorem.

*Theorem 1:* Under A1, A2, there exist matrices $T_i$, $N_i$, $K_i$, $\Pi_i$, for $i = 1, \cdots, M$, such that

$$T_i = I_n - N_i C_i \tag{6}$$

$$\Pi_i = T_i A_i - K_i C_i \tag{7}$$

$$K_i = K_{p_i} - \Pi_i N_i \tag{8}$$

then, the estimation errors become

$$\dot{\tilde{z}} = (T_i A_i - K_i C_i)\tilde{z} + T_i F_i \hat{\omega} - T_i F_i \omega \tag{9}$$

$$\dot{\hat{\omega}} = -K_{I_i} C_i \tilde{z} \tag{10}$$

$$\tilde{\xi} = -L_i \tilde{z} \tag{11}$$

*Proof:* Suppose that the conditions (6), (7) and (8) hold, then the dynamics of the state estimation errors $e_x$ and UI estimation $\hat{\omega}$ become respectively:

$$\tilde{z} = \sum_{i=1}^{M} \alpha_i(\vartheta(t))(z - T_i x) \tag{12}$$

from (3), (5), (6), (7) and (8), the time derivative of (12) gives

$$\dot{\tilde{z}} = \sum_{i=1}^{M} \alpha_i(\vartheta(t))\left((T_i A_i - K_i C_i)\tilde{z} + T_i F_i \hat{\omega} - T_i F_i \omega\right) \tag{13}$$

Let us now consider the time derivative of the unknown input estimation $\hat{\omega}$, from (5) we obtain

$$\begin{aligned} \dot{\hat{\omega}} &= \sum_{i=1}^{M} \alpha_i(\vartheta(t))(K_{I_i}(y - C_i \hat{x})) \\ &= \sum_{i=1}^{M} \alpha_i(\vartheta(t))(K_{I_i} C_i e_x) \end{aligned} \tag{14}$$

where

$$\begin{aligned} e_x &= x - \hat{x} \\ &= \sum_{i=1}^{M} \alpha_i(\vartheta(t))((I_n - N_i C_i - T_i)x - \tilde{z}) \end{aligned} \tag{15}$$

From (6), (15) becomes

$$e_x = -\tilde{z} \tag{16}$$

and from (16), (14) becomes

$$\dot{\hat{\omega}} = \sum_{i=1}^{M} \alpha_i(\vartheta(t))(-K_{I_i} C_i \tilde{z}) \tag{17}$$

which deduce (11). To consider all switches cases, we consider the particular case $\alpha_i(\vartheta(t)) = 1$ and $\alpha_{l \neq i}(\vartheta(t)) = 0$. Then, (13) and (17) become

$$\begin{aligned} \dot{\tilde{z}} &= (T_i A_i - K_i C_i)\tilde{z} + T_i F_i \hat{\omega} - T_i F_i \omega \\ \dot{\hat{\omega}} &= -K_{I_i} C_i \tilde{z} \end{aligned} \tag{18}$$

from (18) the following augmented system is deduced:

$$\begin{aligned} \dot{e}_a(t) &= [A_{ai} - K_{ai} C_{ai}] e_a(t) + F_{ai} \omega(t) \\ \tilde{\xi}(t) &= L_{ai} e_a(t) \end{aligned} \tag{19}$$

where $e_a(t) = \begin{bmatrix} \tilde{z} \\ \hat{\omega} \end{bmatrix}$, $A_{ai} = \begin{bmatrix} T_i A_i & T_i F_i \\ 0 & 0 \end{bmatrix}$, $K_{ai} = \begin{bmatrix} K_i \\ K_{I_i} \end{bmatrix}$, $C_{ai} = \begin{bmatrix} C_i & 0 \end{bmatrix}$, $F_{ai} = \begin{bmatrix} -T_i F_i \\ 0 \end{bmatrix}$ and $L_{ai} = \begin{bmatrix} -L_i & 0 \end{bmatrix}$

The solution $\begin{bmatrix} T_i & N_i \end{bmatrix} \begin{bmatrix} I_n \\ C_i \end{bmatrix} = I$ of (6) depends on the rank of matrix $\begin{bmatrix} I_n \\ C_i \end{bmatrix}$. Since $\begin{bmatrix} I_n \\ C_i \end{bmatrix}$ is of full column rank, a solution of (6) is

$$\begin{bmatrix} T_i & N_i \end{bmatrix} = \begin{bmatrix} I_n \\ C_i \end{bmatrix}^{+} = \left( \begin{bmatrix} I_n \\ C_i \end{bmatrix}^T \begin{bmatrix} I_n \\ C_i \end{bmatrix} \right)^{-1} \begin{bmatrix} I_n \\ C_i \end{bmatrix}^T$$

■

*Remark 2:* The detectability of the $(A_{ai}, C_{ai})$ is equivalent to A2. The proof is detailed in the appendix of [12].

Therefore the switched $H_\infty$ PI observer design problem is reduced to find the proportional $K_{pi}$ and integral $K_{I_i}$ gains such that $[A_{ai} - K_{ai} C_{ai}]$ is a stable matrix for $i = 1, \cdots, M$ and S2 is hold. In order to achieve this objective, consider the following theorem:

*Theorem 2:* Suppose that for all $(i \in \{1, \cdots, M\})$, the pair $(A_{ai}, C_{ai})$ is detectable (see remark 2). If there exist a level of attenuation $\gamma > 0$, a common symmetric positive definite matrix $P \in \mathbb{R}^{(n+n_\omega)\times(n+n_\omega)}$ and matrices $\Gamma_{ai} \in \mathbb{R}^{m\times(n+n_\omega)}$ such that the following inequality is satisfied for $i = 1, \cdots, M$:

$$\min_{P, \Gamma_{ai}} \gamma$$

subject to

$$\begin{bmatrix} A_{ai}^c + C_{ai}^T \Gamma_{ai}^T + \Gamma_{ai} C_{ai} & P F_{ai} & L_{ai}^T \\ F_{ai}^T P & -\gamma^2 I & 0 \\ L_{ai} & 0 & -I \end{bmatrix} < 0 \tag{20}$$

then the switched $H_\infty$ PI observer (5) is obtained. Moreover, the gains $K_{ai}$ of the switched $H_\infty$ PI observer are given by $K_{ai} = \begin{bmatrix} K_i & K_{I_i} \end{bmatrix}^T = -P^{-1}\Gamma_{ai}$ and $A_{ai}^c = A_{ai}^T P + P A_{ai}$.

*Proof:* In order to establish sufficient condition for the existence of (5), satisfying the specifications S1 and S2, the following inequality should be verified

$$\dot{V} + \tilde{\xi}^T \tilde{\xi} - \gamma^2 \omega^T \omega < 0 \tag{21}$$

where $V(e_a(t), t) = e_a^T(t) P e_a(t)$ is the Lyapunov function candidate with $P > 0$. The time derivative of $V(e_a(t), t)$ along the trajectory of system (19) gives

$$\begin{aligned} (21) \quad \Leftrightarrow \quad & \dot{e}_a^T(t) P e_a(t) + e_a^T(t) P \dot{e}_a(t) + \tilde{\xi}^T(t)\tilde{\xi}(t) \\ & -\gamma^2 \omega^T(t)\omega(t) \\ \Leftrightarrow \quad & e_a^T(t)(A_{ai} - K_{ai} C_{ai})^T P e_a(t) + \omega^T(t) F_{ai}^T P e_a(t) \\ & + e_a^T(t) P (A_{ai} - K_{ai} C_{ai}) e_a(t) + e_a^T(t) P F_{ai} \omega(t) \\ & + e_a^T(t) L_{ai}^T L_{ai} e_a(t) - \gamma^2 \omega^T(t)\omega(t) \\ \Leftrightarrow \quad & e_a^T(t)\left[(A_{ai} - K_{ai} C_{ai})^T P + P(A_{ai} - K_{ai} C_{ai}) \right. \\ & \left. + L_{ai}^T L_{ai}\right] e_a(t) + \omega^T(t) F_{ai}^T P e_a(t) \\ & + e_a^T(t) P F_{ai} \omega(t) - \gamma^2 \omega^T(t)\omega(t) < 0 \end{aligned}$$

which can be rewritten as follows

$$\begin{bmatrix} e_a(t) \\ \omega(t) \end{bmatrix}^T \begin{bmatrix} \Delta_{ai} + L_{ai}^T L_{ai} & P F_{ai} \\ F_{ai}^T P & -\gamma^2 I \end{bmatrix} \begin{bmatrix} e_a(t) \\ \omega(t) \end{bmatrix} < 0 \tag{22}$$

where $\Delta_{ai} = (A_{ai} - K_{ai} C_{ai})^T P + P(A_{ai} - K_{ai} C_{ai})$. If follows S1 for any given $\begin{bmatrix} e_a^T(t) & \omega^T(t) \end{bmatrix} \neq 0$ if:

$$\begin{bmatrix} \Delta_{ai} + L_{ai}^T L_{ai} & P F_{ai} \\ F_{ai}^T P & -\gamma^2 I \end{bmatrix} < 0 \tag{23}$$

Using Schur complement, (23) becomes

$$\left[\begin{array}{cc|c} \Delta_{ai} & PF_{ai} & L_{ai}^T \\ F_{ai}^T P & -\gamma^2 I & 0 \\ \hline L_{ai} & 0 & -I \end{array}\right] < 0 \tag{24}$$

Substituting $\Gamma_{ai} = -PK_{ai}$ into (24), (20) is obtained, with $K_{ai} = \left[\begin{array}{cc} K_i & K_{I_i} \end{array}\right]^T = -P^{-1}\Gamma_{ai}$. ■

Finally, the following algorithm summarize all steps required to design a continuous-time switched H$_\infty$ PI observer.

*Algorithm 1:* for all $i \in \{1, \cdots, M\}$

- Compute $\left[\begin{array}{cc} T_i & N_i \end{array}\right] = \left[\begin{array}{c} I_n \\ C_i \end{array}\right]^+$
- Solve the convex optimization problem defined by (20) which gives $K_{ai} = \left[\begin{array}{c} K_i \\ K_{I_i} \end{array}\right] = -P^{-1}\Gamma_{ai}$
- Deduce $\Pi_i = T_i A_i - K_i C_i$ and $K_{p_i} = K_i + \Pi_i N_i$.

## IV. Experimental validation

In this section, an experimental validation of a continuous-time switched H$_\infty$ PI observer is presented. This validation is performed to estimate the road bank and vehicle sideslip angles. The main experimental measurements used for validation are: driver steering angle, longitudinal speed, roll angle, yaw and roll rates. These data are shown by blue curves of Figures 2, 4 and 5. These data are acquired with an instrumented Peugeot 406 vehicle equipped with several sensors like steering angle, accelerometers, Correvit, odometers, gyrometers and four dynamometric hubs. The acquisition device operates at frequency $200\,Hz$.

### A. First scenario: longitudinal speed premise variable

The simulation test is conducted in accordance with the following switching rule using measured longitudinal speed

$$\left\{\begin{array}{llll} V_x = V_{x_1} & \text{and } i=1 & \text{If} & \vartheta \in [V_{x_1}-\Delta, \Delta+V_{x_1}[ \\ V_x = V_{x_2} & \text{and } i=2 & \text{If} & \vartheta \in [V_{x_2}-\Delta, \Delta+V_{x_2}[ \\ V_x = V_{x_3} & \text{and } i=3 & \text{If} & \vartheta \in [V_{x_3}-\Delta, \Delta+V_{x_3}[ \end{array}\right. \tag{25}$$

where $V_{x1} = 36\,km/h$, $V_{x3} = 63\,km/h$, $V_{x3} = 90\,km/h$ and $\Delta = \frac{V_{x_{l+1}} - V_{x_l}}{2}$ for $l = 1, \cdots, 2$ (see switching rule presented in figure 3), then, three local models are obtained $M = 3$ and $i = 1, 2, 3$. The stability of CTSH$_\infty$ PI observer (5) is guaranteed by the resolution of 3 LMIs of theorem 2 to obtain a common Lyapunov matrix $P$ and three matrices $\Gamma_{a1}$, $\Gamma_{a2}$ and $\Gamma_{a3}$.

Figures 4 and 5 show an experimental evaluation of the CT H$_\infty$ PI Observer. All dynamical estimated parameters are close to the measurements like sideslip angle at the CoG, yaw rate, roll angle and roll rate. Figure 5 shows also the estimation of unknown input (road bank angle). However, the poor estimation of the road bank angle can be observed between the abscissa $300\,m$ and $800\,m$. During this phase, the experimental trail is characterized by a sharp braking maneuver as shown by the longitudinal speed of Figure 2 and tire force characteristic of Figure 1. Moreover, the UI attenuation properties of the transfer functions $\left(L_{ai}(pI - (A_{ai} - K_{ai}C_{ai}))^{-1}F_{ai}\right)$ between $\omega$ to $\tilde{\xi}$ for three values of longitudinal speed are presented in Figure 6. Moreover, by computing, $\|\omega\|_2$ and $\left\|\tilde{\xi}\right\|_2 = \left\|\beta - \hat{\beta}\right\|_2$, gives

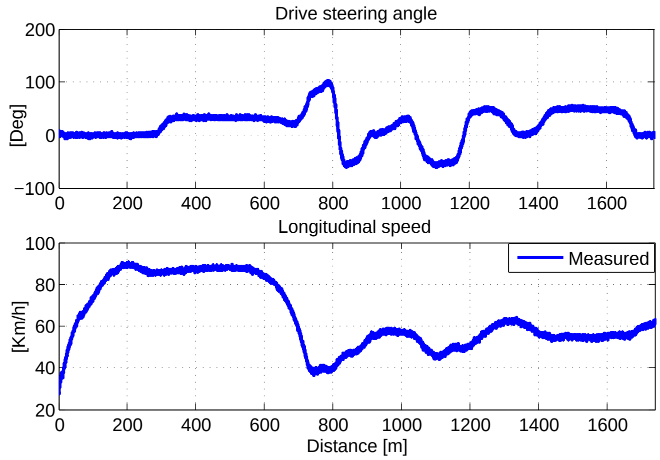


Fig. 2. Measured driver steering angle and longitudinal speed

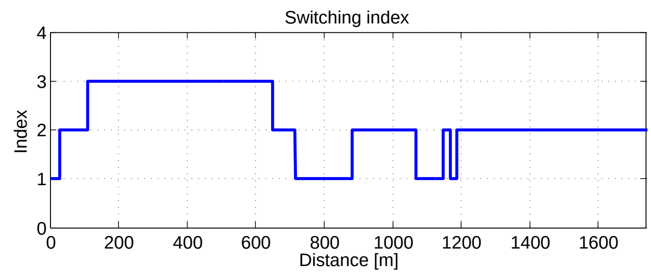


Fig. 3. Switching rule on longitudinal speed

$$\frac{\left\|\tilde{\xi}\right\|_2}{\|\omega\|_2} = 9.538e - 004 < \gamma^* = 2.1 \tag{26}$$

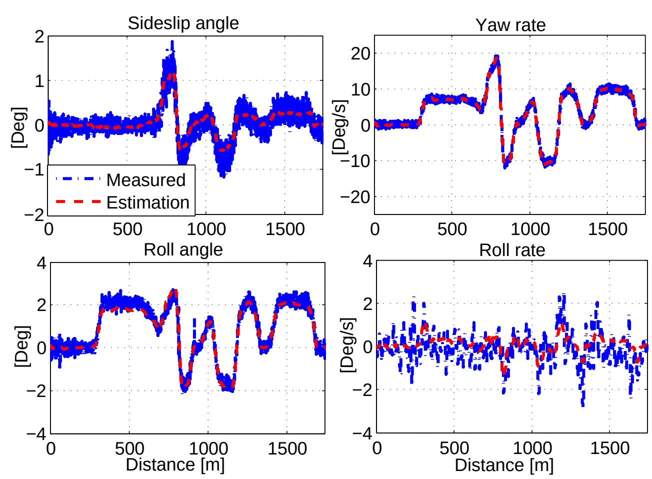


Fig. 4. Sideslip angle, yaw rate, roll angle and roll rate: estimated and measured

To improve this estimation, in the following subsection a switching rules on the cornering stiffnesses $C_f$ and $C_r$ using the approximated front and rear sideslip angles as premise variable.

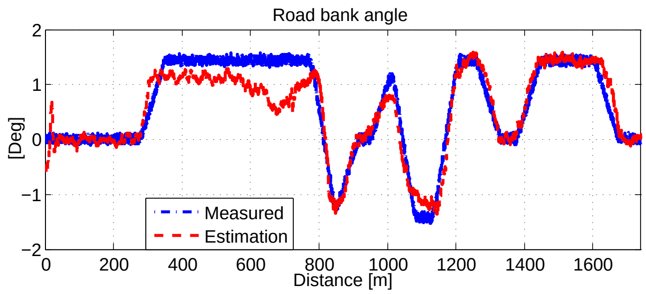


Fig. 5. Road bank angles: estimated and measured

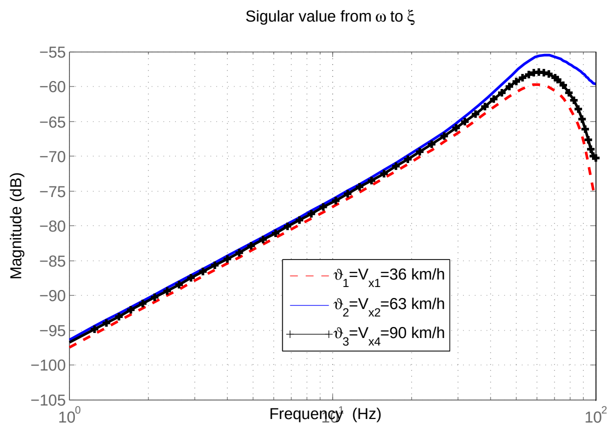


Fig. 6. Transfer function of subsystems $((A_{ai}-K_{ai}C_{ai}), F_{ai}, L_{ai})$, for three values of longitudinal speed, between $\omega$ to $y$

### B. Second scenario: sideslip angle premise variable

For this test, a switching rule on tire cornering stiffnesses is constructed using the approximated front and rear sideslip angle $\alpha_{(f,r)}$ as premise variable as follows:

$$\begin{cases} C_{(f,r)} = C_{(f,r)1} \quad \text{and} \quad i=1 \quad \text{If} \quad \vartheta = \alpha_{(f,r)} < \alpha^* \\ C_{(f,r)} = C_{(f,r)2} \quad \text{and} \quad i=2 \quad \text{If} \quad \vartheta = \alpha_{(f,r)} > \alpha^* \end{cases} \tag{27}$$

with $\alpha^* \approx 0.5\,Deg$ for our case study (see Figure 1). This rule is considered in order to take into account the variation occurred during the braking maneuver displayed on Figure 1. This variation is described by two operating modes, then, two CTSH$_\infty$ PI observers (5) are designed ($M=2$ and $i=1,2$), and their stability is guaranteed by the resolution of 2 LMIs of theorem 2 to obtain a common Lyapunov matrix $P$. The corresponding switching signal is displayed on Figure 7.

Figure 8 shows the road bank angle estimation result. This result is slightly improved between the abscissa $300\,m$ and $800\,m$ by comparing it to the result of Figure 5. This improvement can also be justified by the uses an adequate switching rule. Nevertheless, the estimation results of the dynamical parameters are approximately the same with first scenario. The UI $\omega(t) = \phi_r(t)$ attenuation property subsystems $((A_{ai}-K_{ai}C_{ai}), F_{ai}, L_{ai})$ from $\omega(t)$ to $\tilde{\xi}$ are shown in Figure 9. By computing, $\|\omega\|_2$ and $\left\|\tilde{\xi}\right\|_2 = \left\|\beta - \hat{\beta}\right\|_2$, which gives

$$\frac{\left\|\tilde{\xi}\right\|_2}{\|\omega\|_2} = 8.8542e-003 < \gamma^* = 2.1 \tag{28}$$

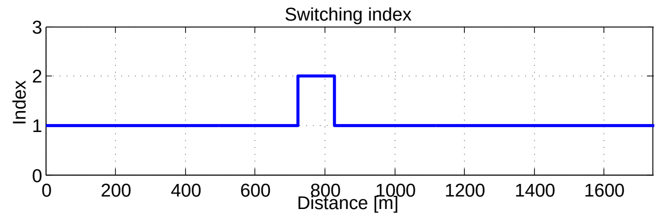


Fig. 7. Switching rule on longitudinal speed

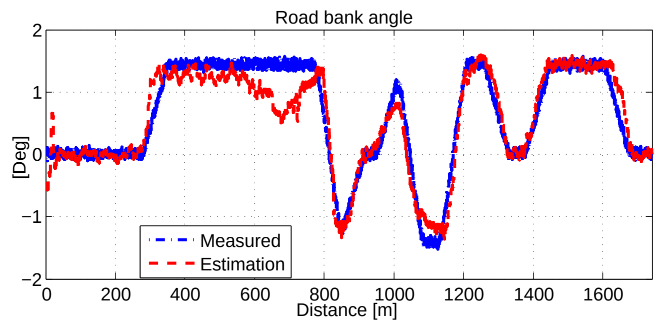


Fig. 8. Road bank angles: estimated and measured

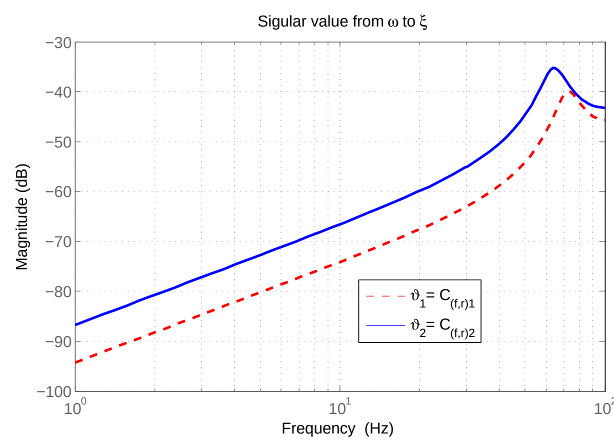


Fig. 9. Transfer function of subsystems $((A_{ai}-K_{ai}C_{ai}), F_{ai}, L_{ai})$ for two values of cornering stiffnesses ($C_{(f,r)1}$ and $C_{(f,r)2}$), between $\omega$ to $y$

It should be pointed out that for two simulation tests, the optimization problem is solved using YALMIP software [20].

## V. Conclusions and Future Work

In this work, design problem of continuous-time switched H$_\infty$ PI observer is addressed. Based on a common Lyapunov function method and H$_\infty$ norm, design method and proofs of global convergence are established. All conditions are expressed in term of the LMIs. This observer is applied on vehicle dynamics to estimate simultaneously the vehicle sideslip angle and the road bank angle (unknown input). Two simulation tests with two switching rules are conducted: for first one, the switching rule is constructed using measured longitudinal speed $V_x(t)$ as premise variable, while for the second one, the switching rule is designed using the approximated front and rear sideslip angles $\alpha(t)$ as premise variable. Simulation results with experimental data show the ability of proposed design method to provide an adequate estimation of state variables and unknown inputs. It should be mentioned that the estimation of sideslip angle is an important step to design efficient safety systems. Moreover, such a variable is used in ESP system which improves the handling and stability of the vehicle. Especially, overcome the use of more expensive sensors like Correvit sensor (around 15 K€) which is currently used to measure such an angle.

To improve the estimation of road bank angles, a switching rule on tire cornering stiffnesses $C_f$ and $C_r$ must be enlarged to the estimated lateral and vertical tire forces. Then, the estimated sideslip and road bank angles could be used in future stabilizing algorithms, particularly for critical situations like understeering and oversteering in curved trajectories which require such data.

## REFERENCES


[1] G. Baffet, A. Charara, and D. Lechner. Estimation of vehicle sideslip, tire force and wheel cornering stiffness. *Control Engineering Practice*, 17(11):1255–1264, 2009.

[2] M.S. Branicky. Multiple lyapunov functions and other analysis tools for switched and hybrid systems. *IEEE Trans. Autom. Control*, 43(4):475–482, 1998.

[3] B. C. Chena and F. C. Hsieha. Sideslip angle estimation using extended kalman filter. *Vehicle System Dynamics: International Journal of Vehicle Mechanics and Mobility*, 46(1):14261431, 2008.

[4] J. Daafouz, P. Riedinger, and C. Iung. Stability analysis and control synthesis for switched systems: A switched lyapunov function approach. *IEEE Trans. Autom. Control*, 47(11):1883–1887, November 2002.

[5] M. Doumiati, A. Charara, A. Victorino, and D. Lechner. *Vehicle Dynamics Estimation using Kalman Filtering: Experimental Validation*. Wiley-ISTE, November 2012.

[6] D. Du, B. Jiang, P. Shi, and S. Zhou. $H_\infty$ filtering of discrete-time switched systems with state delays via switched lyapunov function approach. *IEEE Trans. Autom. Control*, 52:1520–1525, 2007.

[7] L. Fang, H. Lin, and P. J. Antsaklis. Stabilization and performance analysis for a class of switched systems. In *in Proc. 43th IEEE Conf. Decision Control*, pages 3265–3270, 2004.

[8] J.O. Hahn, R. Rajamani, S.H. You, and K.I. Lee. Real-time identification of road-bank angle using differential gps. *IEEE Transaction on control systems technology*, 12(4):589–599, 2004.

[9] L. Imsland, H. F. Grip, T. A. Johansen, T. I. Fossen, J.C. Kalkkuhl, and A. Suissa. On non-linear unknown input observers: applied to lateral vehicle velocity estimation on banked roads. *Int. Jour. of Cont.*, 80:1741–1750, 2007.

[10] N. Kanghyun, O. Sehoon, H. Fujimoto, and Y. Hori. Estimation of sideslip and roll angles of electric vehicles using lateral tire force sensors through rls and kalman filter approaches. *IEEE Transactions on Industrial Electronics*, 60(3):988–1000, 2013.

[11] D. Koenig. Unknown input proportional multiple-integral observer design for linear descriptor systems: Application to state and fault estimation. *IEEE Transactions on Automatic Control*, 50:212–217, 2005.

[12] D. Koenig. Observer design for unknown input nonlinear descriptor systems via convex optimization. *IEEE Transactions on Automatic Control*, 51(6):p1047–1052, 2006.

[13] D. Koenig and S. Mammar. Design of proportional-integral observer for unknown input descriptor system. *IEEE Transactions on Automatic Control*, 47:2057–2062, 2002.

[14] D. Koenig and B. Marx. $h_\infty$ filtering and state feedback control for discrete-time switched descriptor systems. *IET control theory & applications*, 3(6):661–670, 2009.

[15] D. Koenig, B. Marx, and D. Jacquet. Unknown input observers for switched nonlinear discrete time descriptor systems. *IEEE Trans. Autom. Control*, 53:373–379, 2008.

[16] D. Liberzon and A. S. Morse. Basic problems in stability and design of switched system. *IEEE Control Syst. Mag.*, 19(5):59–70, Oct. 1999.

[17] H. Lin and P. J. Antsaklis. Switching stabilization and $l_2$ gain performance controller synthesis for discrete-time switched linear systems. In *45th IEEE Conf. Decision Control*, pages 2673–2678, 2006.

[18] H. Lin and P. J. Antsaklis. Switching stabilizability for continuous-time uncertain switched linear systems. *IEEE Trans. Autom. Control*, 52(4):633–646, 2007.

[19] H. Lin and P. J. Antsaklis. Stability and stabilizability of switched linear systems: A survey of recent results. *IEEE Trans. Autom. Control*, 54(2):308–321, 2009.

[20] J. Löfberg. Yalmip : A toolbox for modeling and optimization in MATLAB. In *Proceedings of the CACSD Conference*, Taipei, Taiwan, 2004.

[21] L. Menhour, D. Koenig, and B. d'Andréa Novel. Road bank and vehicle roll angles estimation based on proportional-integral observer. In *8th IFAC Symposium SAFEPROCESS-2012, Mexico City*, August 29-31 2012.

[22] S. Prajna and A. Papachristodoulou. Analysis of switched and hybrid systemsbeyond piecewise quadratic methods. In *in Proc. 42th IEEE Conf. Decision Control*, pages 2779–2784, 2003.

[23] Y. Sebsadji, S. Glaser, S. Mammar, and M. Netto. Vehicle roll and road bank angles estimation. In *in Proceedings of the 17th IFAC World Congress, Seoul, Korea*, July 6-11 2008.

[24] J. Stephant, A. Charara, and D. Meizel. Virtual sensor, application to vehicle sideslip angle and transversal forces. *IEEE Transactions on Industrial Electronics*, 51:pp. 278–289, 2004.

[25] Z. Sun and S. S. Ge. Analysis and synthesis of switched linear control systems. *Automatica*, 41:181–195, 2005.

[26] L. Xie. Output feedback $h_\infty$ control of systems with parameter uncertainty. *Int. J. Control*, 63:741–750, 1996.

[27] H. Xu, Y. Zou, and S. Xu. Robust $h_\infty$ control for a class of uncertain nonlinear two-dimensional systems. *Int. J. Innovative Comput. Inf. Control*, 1:181–191, 2005.

[28] S. You, J. Hahn, and H. Lee. New adaptive approaches to real-time estimation of vehicle sideslip angle. *Control Engineering Practice*, 17(12):13671379, 2009.


TABLE I

NOTATIONS

| Symbol | Variable name |
|---|---|
| $V_x$ | longitudinal speed $[km.h]$ |
| $\dot{\psi}$, $\psi$ | yaw rate $[rad/s]$ and yaw angle $[rad]$ |
| $\dot{\phi}_v$, $\phi_v$ | roll rate $[rad/s]$ and vehicle roll angle $[rad]$ |
| $\beta$, $\delta$ | sideslip angle at the CoG $[rad]$ and wheel steer angle $[rad]$ |
| $\phi_r$ | road bank angle $[rad]$ |
| $F_{yf}$, $F_{yr}$ | front and rear lateral forces in the vehicle coordinate $[N]$ |
| $L_f$, $L_r$ | distances from the CoG to the front and rear axles $[m]$ |
| $h_r$ | distance between the roll center and the CoG $[m]$ |
| $I_z$ | yaw moment of inertia $[kg.m^{-2}]$ |
| $I_x$ | moment of inertia about $x$ axis $[kg.m^2]$ |
| $C_f$, $C_r$ | front and rear cornering stiffnesses $[N/rad]$ |
| $K_r$ | roll stiffness coefficient $[N.m.rad^{-1}]$ |
| $b_r$ | roll damping coefficient $[N.m.s.rad^{-1}]$ |
| $\alpha_f$, $\alpha_r$ | front and rear tire slip angles $[rad]$ |
| $g$, $m$ | acceleration due to gravity $[m/s^2]$ and vehicle mass $[kgm^2]$ |
| $(.)^T$ | stands for the transpose matrix |
| $(.) > 0$ | symmetric positive definite matrix |
| $(.)^+$ | pseudoinverse matrix of Moore-Penrose |